Comparisons of Statistics for Wind Speeds Around an Isolated Building Determined by Wind-tunnel Experiment and Numerical Simulation

T. Tong
Interdisciplinary Graduate School of Engineering Sciences, Kyushu University

Y. Li
Interdisciplinary Graduate School of Engineering Sciences, Kyushu University

W. Wang
Interdisciplinary Graduate School of Engineering Sciences, Kyushu University

Ikegaya, Naoki
Interdisciplinary Graduate School of Engineering Sciences, Kyushu University

https://doi.org/10.5109/7323337

出版情報：Proceedings of International Exchange and Innovation Conference on Engineering & Sciences (IEICES). 10, pp.692-699, 2024-10-17. International Exchange and Innovation Conference on Engineering & Sciences
バージョン：

Comparisons of Statistics for Wind Speeds Around an Isolated Building Determined by Wind-tunnel Experiment and Numerical Simulation

T. Tong[1], Y. Li[1,2], W. Wang[1,2], N. Ikegaya[1,2]

[1] Interdisciplinary Graduate School of Engineering Sciences, Kyushu University, Japan,
[2] Faculty of Engineering Sciences, Kyushu University, Japan,

Corresponding author email: tongt@kyudai.jp

Abstract: *Accurately predicting low-occurrence wind speeds around urban structures is vital for proper building design as well as pedestrian safety. Although Large-eddy simulation (LES) is often used as a high-fidelity model compared to Reynolds-averaged Navier–Stokes (RANS) simulation, current validation processes mainly compare fundamental statistics of the mean and standard deviations of the wind speed. Discrepancies between LESs and wind-tunnel experiments (WTE) remain unclear, particularly regarding physical quantities that characterize the unsteadiness of turbulent flows, such as probability densities, power spectral densities, and high-order moments of the wind speed. This study evaluates LES's results in predicting unsteady wind behavior around a 1:1:2 block model. Two advection schemes in LESs, including first-order upwind and second-order linear were investigated. The results show notable discrepancies, particularly in high-order statistics with WTE consistently exhibiting higher energy levels across all frequencies. These findings underscore the need to refine numerical models to improve their predictive accuracy.*

Keywords: Large-eddy simulation; Wind-tunnel experiment; High-order moment; Probability density; Power spectral density

1. INTRODUCTION

Ensuring the accurate prediction of low-occurrence wind speeds in urban settings is vital for the safety and design of structures. The ability to model wind flows accurately around buildings can significantly mitigate potential hazards and enhance architectural design efficiency. Computational Fluid Dynamics (CFD) techniques have thus become indispensable tools, providing detailed simulations of complex airflow patterns. Despite the widespread use of Reynolds-averaged Navier-Stokes (RANS) models, they often struggle to capture the intricate and unsteady nature of turbulent flows [1], [2], [3]. LES has proven to be a superior alternative due to its ability to model unsteady flows more accurately than RANS. This method has been recognized for its effectiveness in capturing detailed turbulence structures and improving predictive accuracy in urban wind environments [4], [5], [6]. However, the integration and application of LES require rigorous sensitivity studies and validation processes. The AIJ guidelines and the European COST Action 732 have established robust frameworks for CFD simulations using RANS, but the growing body of academic and practical studies underscores the need for further refinement and validation of LES models [1], [3], [7].

Numerous studies have highlighted the advantages of LES over RANS models in simulating urban wind environments. For instance, Hertwig et al. [8], [9] conducted extensive LES studies around realistic urban structures, demonstrating significant improvements in predicting wind speed distributions compared to traditional RANS models. Also, research by Gousseau et al. [10] and Okaze et al. [11] revealed that LES effectively captures detailed flow fields around simplified block models, even with varying grid resolutions and sub-grid scale (SGS) models. These findings emphasize the potential of LES in enhancing the reliability of wind environment assessments [12], [13]. Furthermore, studies by He and Song [6] and Tamura [5] demonstrated LES's capability to predict complex flow patterns in realistic urban settings. The work of Abd Razak et al. [14] and Ikegaya et al. [15] further validated LES's proficiency in simulating airflow around simplified block models, reinforcing its robustness across diverse urban configurations.

The increasing application of LES for both realistic and generic building configurations has highlighted the need for establishing comprehensive guidelines for its usage. Hertwig et al. [8], [9] conducted extensive studies on LES prediction accuracy by comparing fundamental statistics and turbulent scales within and above canopies for realistic building arrays. Similarly, Ikegaya et al. [16] performed a series of sensitivity studies on advection schemes to reproduce turbulent flow fields around a 1:1:2 block model. Although the significance of advection schemes and the effects of numerical viscosity have been well documented in RANS guidelines (such as the AIJ guidelines), systematic comparisons of turbulent statistics, probability densities, and power spectra underscore the critical role of advection schemes in LES. Following this, Okaze et al. [17] reported a comprehensive sensitivity study on various numerical conditions in LES for airflow around a 1:1:2 block model. Their study covered mesh resolutions, advection schemes, turbulence models, and convergence criteria, providing a robust framework for establishing LES guidelines.

Despite the advancements in LES and numerous sensitivity studies on its practical use for unsteady simulations, accurately predicting the unsteadiness of the flow remains a significant challenge. It is widely accepted that LES can reproduce more accurate flow patterns around buildings than RANS simulations, particularly regarding fundamental statistics. However, the validation of LES in capturing unsteadiness is still insufficient. High-order turbulent statistics, which are significantly affected by rare wind events [18], low-occurrence wind events, probability density distributions, and power spectral densities, have not been thoroughly compared between simulations and experiments. Studies by Wang et al. [18] and Li et al. [19] have highlighted that although LES can accurately predict mean flow characteristics, it often fails to replicate higher-order moments and low-occurrence values. Furthermore, Ikegaya et al. [16] examined the impact of advection schemes on probability and power spectral densities through a systematic comparison of different percentages of the upwind advection scheme. However, they did not identify the best scheme for reproducing experimental results. Therefore, further validation against experimental data is necessary to discuss the accuracy of LES in capturing flow unsteadiness comprehensively.

This study aims to tackle these challenges by conducting a detailed comparison between wind-tunnel experiments (WTE) and LES results for a 1:1:2 block model. By analyzing various parameters such as velocity profiles, skewness, kurtosis, and other statistics, we seek to assess the effectiveness of LES in replicating low-occurrence wind conditions [20], [21]. The comparative analysis will provide insights into the strengths and limitations of LES in urban wind simulations, highlighting areas where numerical models can be refined to enhance predictive accuracy. This research will contribute to a better understanding of LES capabilities and pave the way for more reliable wind environment assessments in urban settings [4], [5].

One important factor affecting the accuracy of LES is the choice of numerical schemes, especially advection schemes, as examined in the work of Ikegaya et al [16]. Studies have demonstrated that numerical viscosity plays a significant role in reproducing turbulent flows. Higher numerical viscosity in first-order upwind schemes tends to underpredict turbulent kinetic energy and mean velocities. In contrast, second-order central schemes and their hybrids align more closely with experimental data [11], [22], [23]. For example, research by Ono et al. [24] and Salim et al. [25] stated the impact of different advection schemes on the accuracy of turbulence statistics in LES simulations. This study builds on these findings by evaluating the performance of various advection schemes in predicting low-occurrence wind speeds and high-order turbulent statistics around a block model. Through comprehensive comparative analysis, our goal is to enhance the predictive capabilities of CFD simulations and support safer urban design practices [24], [25]. By integrating data from both WTE and LES, this study aims to provide valuable insights into the current capabilities and limitations of numerical methods in simulating urban wind environments.

This paper is structured as follows: Section 2 describes the methodology, including the setup for both WTE and LES. Section 3 presents the results, highlighting the comparison of mean, standard deviation, skewness, kurtosis, fifth- and sixth-order moments as well as the PDF and PSD comparison between the experimental and numerical data at a specific probe point. Finally, Section 4 provides conclusions and suggestions for future research, emphasizing the need for continued refinement of LES models to improve their predictive accuracy for low-occurrence wind events in urban environments.

2. METHODOLOGY

2.1 Description of the wind tunnel experiment

Table 1 provides detailed information about the WTE conducted at Tokyo Polytechnic University's open-circuit wind tunnel, under the supervision of the Wind Engineering Institute Co., Ltd. The experimental setup and procedures were consistent with previous studies documented in the CFD database of Tokyo Polytechnic University [26], [27]. The wind tunnel's measurement section dimensions were 14.0 m in the streamwise direction, 1.2 m in the spanwise direction, and 1.0 m in the vertical direction. The streamwise lengths of the approaching and test sections were 11.2 m and 2.8 m, respectively. Within the test section, a 1:1:2 single block model with a block height of H = 0.2 m was positioned at downstream from the streamwise end of the approaching section. Turbulent inflow to the test section was generated using various turbulence generators, including barriers, spires, and roughness elements, to replicate a turbulent boundary layer with a power law index of approximately 0.27. The Reynolds number, calculated based on H and the mean wind velocity of the approaching flow at the building height u_H, was 4.3×10^4. Velocity components were measured at various locations using split-film fiber probes (SFP, DANTEC 55R55 for streamwise, 55R57 for lateral, and 55R56 for vertical components). These probes can simultaneously detect two-directional velocity components when the wind direction is constant or one-directional velocity components when the wind direction is variable. Thus, SFPs were used to determine all three velocity components by conducting three separate measurements with directions perpendicular to the flow at each position around the single block model. For the approaching flow measurement, where the wind direction is primarily determined by the streamwise velocity component, two velocity components were measured to determine the correlation terms (e.g., $\overline{u'w'}$, where u and w are the streamwise and vertical velocity components, u' and w' are their fluctuation parts, and the overbar indicates the temporal average). The sampling duration and frequency were set at 60 s and 1000 Hz, respectively.

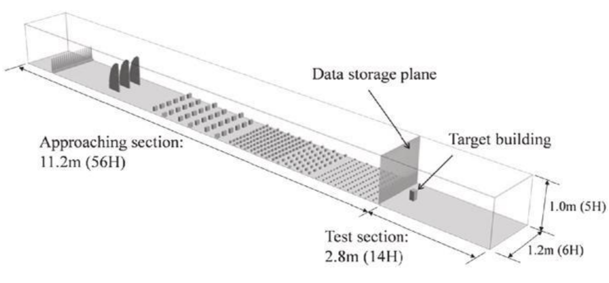

Fig. 1. Features of the single-block model [17].

Table 1. Details of wind-tunnel experiment [16], [17]

Item	Content
Aspect ratio of building (length: width: height)	1:1:2
Height of building (m)	0.2
Reynolds number	4.3×10^4
Cross-sectional dimension of wind tunnel (m)	1.2 (spanwise)×1.0 (vertical)
Streamwise length of approaching section (m)	11.2
Amount of measurement points	181 (vertical plane $y = 0$) 150 (horizontal plane $z = H/16$)
Sampling frequency (Hz)	1000
Sampling duration (s)	60

2.2 Numerical Settings

LESs were conducted to analyze the wind fields around a 1:1:2 single block model with a height of H = 0.2 m using the finite volume method implemented in OpenFOAM v1606+ [21]. Fig. 2 illustrates the schematic diagram of the computational domain. The coordinates were defined as *x*, *y*, and *z* for the streamwise, spanwise, and vertical directions, respectively. The resolved-scale velocities were denoted as *u*, *v*, and *w*. The computational domain for the numerical simulation was set as 12.5H in the streamwise direction, 6.0H in the spanwise direction, and 5.0H in the vertical direction, where H represents a characteristic length scale. These dimensions were consistent with those used in the WTE [20]. The Standard Smagorinsky model [28] with a Smagorinsky constant (C_S = 0.12) was employed as the turbulence model. Orthogonal grids were used, with a minimum size of H/40 near the block surfaces which was chosen based on the grid-sensitivity study in the previous study by Ozake et al. [11]. A no-slip wall boundary condition was applied, using the Spalding wall function [29] on the top, bottom, sides as well as block surfaces. For the inlet boundary condition, turbulence inflow generated in a precursor simulation was used [17], while an advective boundary condition was applied at the outlet. The simulation utilized a time step of 1.0×10^{-4} s, with a sampling duration of 120 s and a sampling interval of 1.0×10^{-3} s. The PISO algorithm [29] was implemented for the simulation with a convergence tolerance of 1.0×10^{-7}. Table 2 lists the general numerical settings for all cases.

This study tested static spatial discretization schemes for the advection term. The interpolation scheme used in this study was a combination of the first-order upwind interpolation scheme and the second-order linear interpolation scheme. The blending ratios β represents the percentage of upwind scheme, which were 0% and 100% in this study. The case name of the advection term is denoted as Linear 100% as C100, and Upwind 100% as U100.

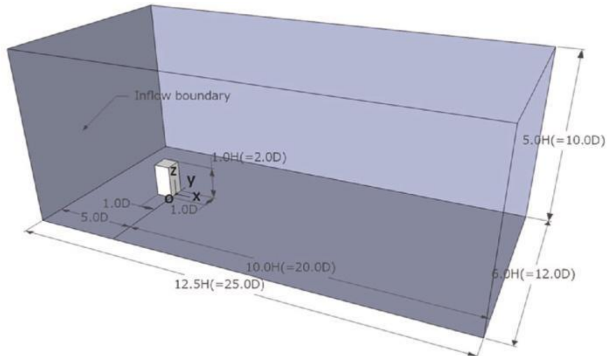

Fig. 2. Schematic of the numerical setup for LES [17].

Table 2. General numerical conditions for all cases

Item	Content
Computational domain	12.5H (streamwise) ×6.0H (spanwise) ×5.0H (vertical)
Turbulence model	Standard Smagorinsky model (Smagorinsky constant C_S = 0.12)
Computational grids	Orthogonal grid
Minimum grid	$H/40$ (Grid20)
Wall boundary condition	No-slip walls by Spalding wall function (top, bottom, sides and block surfaces)
Inlet boundary condition	Turbulence inflow generated in a precursor simulation
Outlet boundary condition	Advective boundary condition
Time step (s)	1.0×10^{-4}
Sampling time (s)	120
Sampling interval (s)	1.0×10^{-3}
Algorithm	PISO algorithm
Tolerance	1.0×10^{-7}

3. RESULTS AND DISCUSSION

3.1 Inflow condition

Fig. 3 illustrates the comparison of vertical profiles for statistics determined by the turbulent velocity used as the inflow boundary condition and those measured at the same position in the WTE. Here, $\underline{u}$, $\underline{v}$ and $\underline{w}$ represent the temporal mean of each directional wind velocity component, respectively, and u', v' and w' are the fluctuations of the wind velocity component in each corresponding direction, respectively, defined as $u' = u - \underline{u}$, $v' = v - \underline{v}$, and $w' = w - \underline{w}$. The standard deviations of each directional wind velocity component are defined as $\sigma_u = \sqrt{\underline{u'^2}}$, $\sigma_v = \sqrt{\underline{v'^2}}$, and $\sigma_w = \sqrt{\underline{w'^2}}$. The high-order moments, i.e. skewness, kurtosis, fifth- and sixth-order moment of the three wind velocity components, are defined as $Sk_i = \underline{i'^3}/\sigma_i^3$, $Kt_i = \underline{i'^4}/\sigma_i^4$, $m5_i = \underline{i'^5}/\sigma_i^5$, and $m6_i = \underline{i'^6}/\sigma_i^6$, where $i = u, v, w$. The convergence of these higher-order statistics was confirmed in Wang et al. [18]. The mean and standard deviations were normalized by the reference wind velocity u_{ref}, which refers to the mean streamwise velocity of the approaching flow at $x/H = -3.0$, $y/H = 0$, and $z/H = 1.0$.

In Fig. 3(a), the mean streamwise velocity predicted by LES shows good agreement with the experimental results.

However, the standard deviations of the velocities in the three directions in the LES are slightly smaller compared to those in the WTE. As reported by Ikegaya et al. [16], the exact reason for this overestimation is not identified; however, it is likely due to the inflow conditions at the uppermost inlet of the precursor simulations, where a laminar flow is provided.

Regarding the skewness of v, both WTE and LES results are nearly zero due to the spanwise geometric symmetry at the measurement location ($y = 0$). In contrast, the skewness of u transitions from positive to negative as height increases, while w exhibits the opposite trend. Though the differences of Sk_u between WTE and LES results are higher at high locations ($z/H > 2$) than those at low locations ($z/H < 2$), the skewness of the streamwise component is well reproduced in the LES. The skewness of the vertical component, however, is less accurately predicted, likely due to the very weak magnitude of the skewness values. A similar trend of large differences at higher locations is observed in the prediction of kurtosis. This discrepancy is possibly due to insufficient grid resolution at higher locations, which fails to capture high-frequency turbulent structures accurately, leading to inaccuracies in higher-order statistics predictions. Nevertheless, in this study, data collected at probe points were used only up to heights of $z/H \leq 1.5$. Additionally, kurtosis serves as an index to show the deviation of the probability distribution function from a Gaussian distribution, categorizing the distribution characteristics as either softened ($Kt_i > 3$) or hardened ($Kt_i < 3$). In terms of these categorizations, the kurtosis in LES is well reproduced. Overall, in the lower regions, the skewness and kurtosis results for all three velocity components show good agreement with the WTE results.

3.2 Low-order statistics

In Fig. 4, the normalized mean and standard deviation of the three wind velocity components are illustrated for the vertical plane. For the mean wind velocities, most of the scatters in two cases are distributed along the solid diagonal line, while for the standard deviation, almost all data are distributed below the solid diagonal line, indicating that LESs underestimate the results. However, for the standard deviation, most data in C100 are distributed within in the deviation range from -50%, and 200%. Although the mean wind velocities can be accurately simulated using the U100 advection scheme, the standard deviations calculated using U100 generally exhibit obvious disparities compared to the results obtained from WTEs, particularly concerning the spanwise wind velocity component as reported by Ikegaya et al. [16]. This might be caused by the numerical dissipation inherent in the first-order upwind scheme when handling the sharp gradients in the flow field, especially around vortex structures. Although these analyses were already performed in Okaze et al. [17] and Ikegaya et al. [16], the deviation of the fundamental statistics were shown in this section as a reference for the following discussion on the high-order statistics.

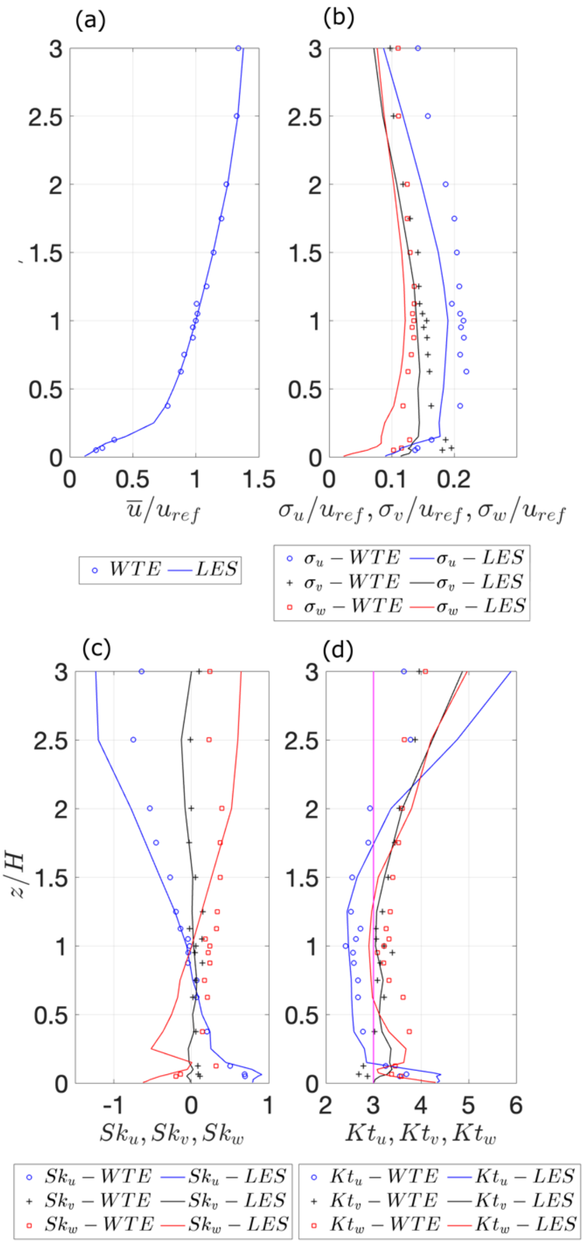

Fig. 3. Vertical profiles for (a) streamwise velocity, (b) standard deviations, (c) skewness and (d) kurtosis determined by the turbulent velocity used as the inflow condition at the vertical plane $y/H = 0$. Lines: LES data used as the inlet boundary condition. Symbols: WTE data

3.3 High-order statistics

Fig. 5 and 6 present the comparison between the results of WTEs and LESs for the skewness, kurtosis, fifth- and sixth-order moments of the streamwise, spanwise, and vertical velocity components at $y/H = 0$ plane, respectively. As implemented in the statistical models [30], [31], the accuracy of the high-order statistics is crucial for predicting low-occurrence wind speeds. The high-order statistics, including skewness, kurtosis, fifth- and sixth-order moments, show less agreement between the WTE and LES results compared to the agreement observed in the low-order statistics, as shown in Fig. 5. Specifically, for the odd-order moments (skewness and fifth-order moment), the relationship between the WTE and LES results deviates significantly from the 0% difference line, with disparities even ranging out of the 200% and -50% differences for all three wind velocity components. Conversely, for the even-order moments (kurtosis and sixth-order moment), almost all scatters are located within the range between 200% and -50% differences (acceptable range).

The discrepancy between the results of odd- and even-order moments may be attributed to the inherent characteristics of these moments. Even-order moments are generally influenced by symmetry, while odd-order moments capture the asymmetry of the distribution. As a result, even-order moments tend to show better agreement with experimental data, whereas the asymmetry reflected in odd-order moments can lead to greater differences between WTE and LES results. Previous research by Wang et al. [18] also indicated that odd-order moments require a longer sampling duration to achieve convergence compared to even-order moments. Nevertheless, it remains unclear whether the discrepancies observed in the current study are due to the sampling duration needed to determine the higher-order statistics.

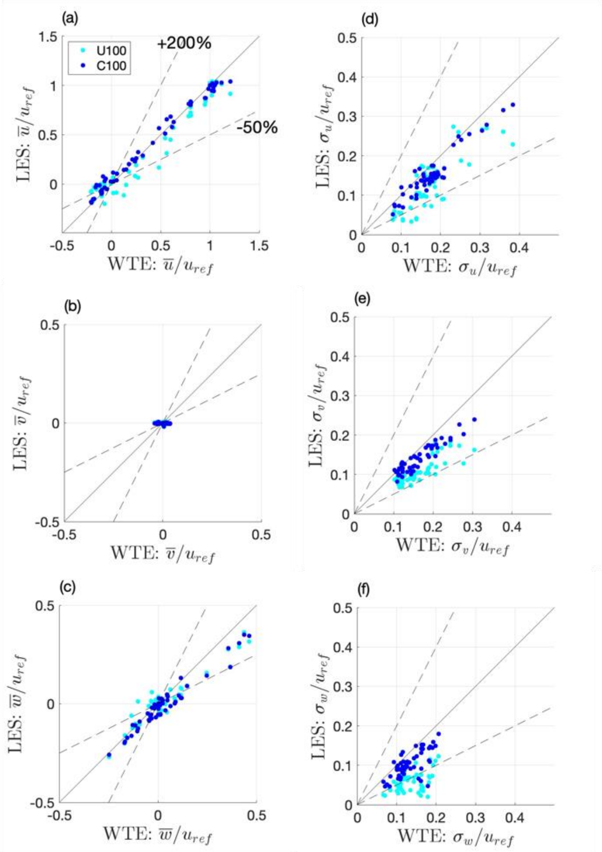

Fig. 4. Comparison between the results of WTEs and LESs for the mean and standard deviation of (a, d) streamwise, (b, e) spanwise and (c, f) vertical velocity components at $y/H = 0$. The solid and dashed diagonal lines indicate the 0%, -50%, and 200% differences.

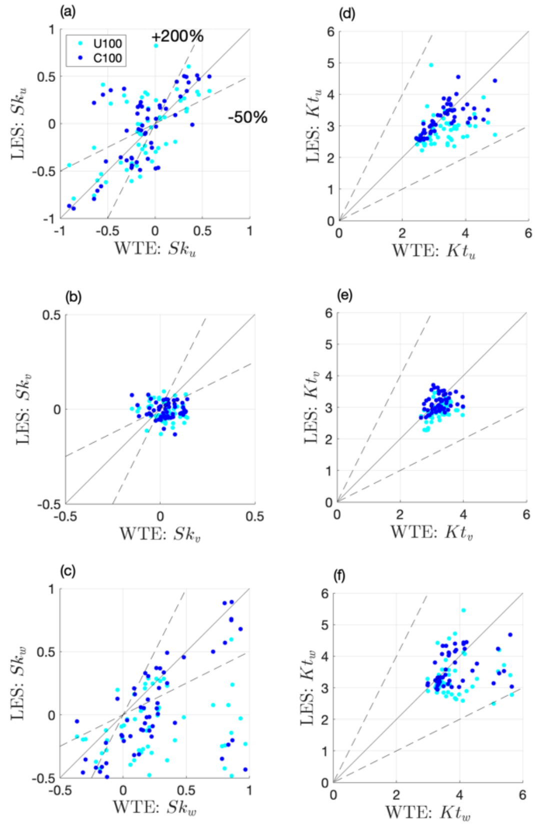

Fig. 5. Comparison between the results of WTEs and LESs for the skewness and kurtosis of (a, d) streamwise, (b, e) spanwise, and (c, f) vertical velocity components at $y/H = 0$. The solid and dashed diagonal lines indicate the 0%, -50%, and 200% differences.

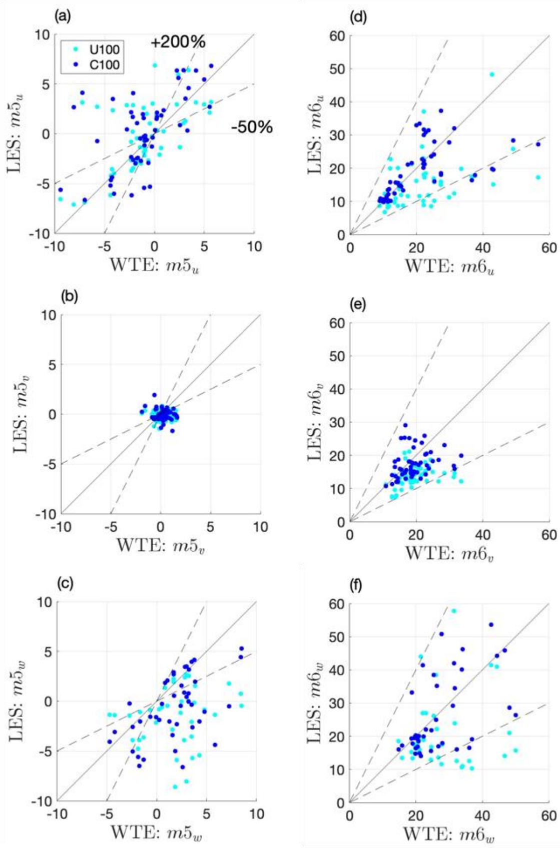

Fig. 6. Comparison between the results of WTEs and LESs for the fifth- and sixth-order moment of (a, d) streamwise, (b, e) spanwise, and (c, f) vertical velocity components at $y/H = 0$. The solid and dashed diagonal lines indicate the 0%, -50%, and 200% differences.

3.4 Probability density function and power spectral density

This section presents and compares the results of probability density function (PDF) and power spectral density (PSD) between the WTE and LESs at a typical probe point at the coordinate of $x/H = 0.05, y/H = 0, and\ z/H = 1.125$. The PDFs are normalized by the $\underline{u_i}^{C100}$ and ${\sigma_{u_i}}^{C100}$, where $\underline{u_i}^{C100}$ and ${\sigma_{u_i}}^{C100}$ are the mean and standard deviation of the velocity component u_i for C100 by following Ikegaya et al. [16]. The power spectral densities S_{u_i} for the wind velocity component u_i and the frequency f are normalized as $S_{u_i}f/{u_{ref}}^2$ and fH/u_{ref} respectively by using a velocity scale of u_{ref} and length scale H. The PSDs were smoothed using a Gaussian-type smoothing function with a bandwidth of 1 Hz applied to the original data.

Fig. 7 and 8 describes the distributions of PDF and PSD for the streamwise, spanwise, and vertical wind velocity components, respectively, at the coordinate of $x/H = 0.05$, $y/H = 0$, and $z/H = 1.125$, which is located on the leeward side of the block building. Due to flow recirculation and reattachment, the PDFs for the streamwise wind velocity component exhibit a negative skew, while the PDFs for the vertical velocity component display a positive skew. Those phenomena are accurately captured by the C100 in general rather than the U100. For three wind velocity components, the WTE data shows a broader distribution, indicating higher velocity fluctuations and turbulence intensity, whereas the U100 one is more concentrated, reflecting the limitations of LES in capturing high-intensity turbulence phenomena.

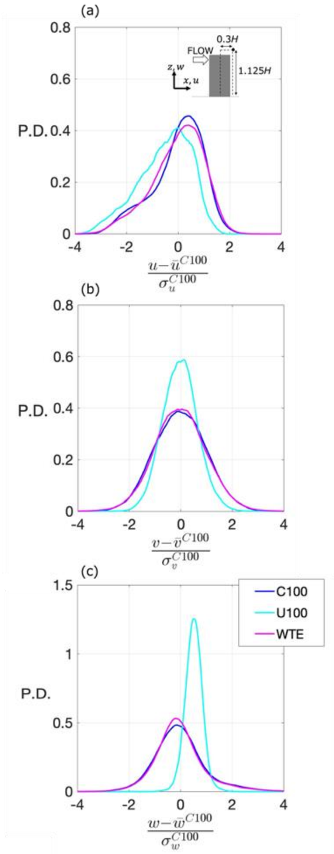

Fig. 7. The probability density function for (a) the streamwise, (b) spanwise, and (c) vertical velocity components at ($x/H = 0.05$, $y/H = 0$, and $z/H = 1.125$).

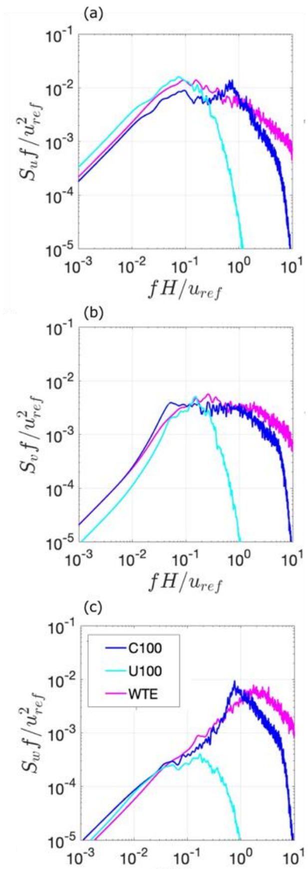

Fig. 8. The power spectral density for (a) the streamwise, (b) spanwise, and (c) vertical velocity components at ($x/H = 0.05$, $y/H = 0$, and $z/H = 1.125$).

4. CONCLUSION

This study employs a comprehensive methodology to compare LES and WTE in predicting low-occurrence wind speeds and turbulent statistics around a 1:1:2 block model. The analysis includes the examination of two advection schemes: first-order upwind (U100) and second-order linear (C100).

The findings reveal that LES, especially with the C100 advection scheme, closely matches the mean velocity profiles of WTE. However, LES struggles to accurately replicate higher-order statistics such as skewness and kurtosis, particularly at higher altitudes where grid resolution limitations affect turbulence representation.

The analysis of Probability Density Function (PDF) and Power Spectral Density (PSD) further highlighted the limitations of LES in capturing high-intensity turbulence phenomena. The WTE data exhibited broader distributions, indicating higher velocity fluctuations and turbulence intensity, which LES, particularly with the U100 scheme, failed to reproduce accurately.

Despite these challenges, LES remains a valuable tool for urban wind simulations. Future research should focus on improving numerical schemes and grid resolutions to better capture low-occurrence wind events and high-order turbulent statistics, ultimately contributing to safer and more efficient urban design practices.

Acknowledgements
This study employs the datasets obtained by the working group of the CFD Evaluation Benchmark Tests, Architectural Institute of Japan. The authors express their gratitude to tis member for providing the velocity fields data for this analysis.

5. REFERENCES

[1] J. Franke, A. Hellsten, K. H. Schlünzen, and B. Carissimo, "The COST 732 Best Practice Guideline for CFD simulation of flows in the urban environment: A summary," *Int J Environ Pollut*, vol. 44, no. 1–4, 2011, doi: 10.1504/IJEP.2011.038443.

[2] R. Yoshie *et al.*, "Cooperative project for CFD prediction of pedestrian wind environment in the Architectural Institute of Japan," *Journal of Wind Engineering and Industrial Aerodynamics*, vol. 95, no. 9–11, 2007, doi: 10.1016/j.jweia.2007.02.023.

[3] M. Schatzmann, H. Olesen, and J. Franke, *Cost 732 Model Evaluation Case Studies : Approach and Results*, no. 732. 2010.

[4] S. Murakami, A. Mochida, and Y. Hayashi, "Examining the κ-ϵ model by means of a wind tunnel test and large-eddy simulation of the turbulence structure around a cube," *Journal of Wind Engineering and Industrial Aerodynamics*, vol. 35, no. C, 1990, doi: 10.1016/0167-6105(90)90211-T.

[5] T. Tamura, "Towards practical use of LES in wind engineering," *Journal of Wind Engineering and Industrial Aerodynamics*, vol. 96, no. 10–11, 2008, doi: 10.1016/j.jweia.2008.02.034.

[6] J. He and C. C. S. Song, "Evaluation of pedestrian winds in urban area by numerical approach," *Journal of Wind Engineering and Industrial Aerodynamics*, vol. 81, no. 1–3, 1999, doi: 10.1016/S0167-6105(99)00025-2.

[7] H. Osman, M. A. Zainol, and N. Ikegaya, "Statistical analysis of turbulent flow over a building array using LES," in *International Exchange and Innovation Conference on Engineering and Sciences*, 2023. doi: 10.5109/7158035.

[8] D. Hertwig, G. Patnaik, and B. Leitl, "LES validation of urban flow, part II: eddy statistics and flow structures," *Environmental Fluid Mechanics*, vol. 17, no. 3, 2017, doi: 10.1007/s10652-016-9504-x.

[9] D. Hertwig, G. Patnaik, and B. Leitl, "LES validation of urban flow, part I: flow statistics and frequency distributions," *Environmental Fluid Mechanics*, vol. 17, no. 3, 2017, doi: 10.1007/s10652-016-9507-7.

[10] P. Gousseau, B. Blocken, and G. J. F. Van Heijst, "Quality assessment of Large-Eddy Simulation of wind flow around a high-rise building: Validation and solution verification," *Comput Fluids*, vol. 79, 2013, doi: 10.1016/j.compfluid.2013.03.006.

[11] T. Okaze et al., "Large-eddy simulations of flow around a high-rise building: validation and sensitivity analysis on turbulent statistics," in *7th European-African Conference on Wind Engineering*, 2017.

[12] O. Coceal, A. Dobre, T. G. Thomas, and S. E. Belcher, "Structure of turbulent flow over regular arrays of cubical roughness," *J Fluid Mech*, vol. 589, 2007, doi: 10.1017/S002211200700794X.

[13] Y. Tominaga, A. Mochida, S. Murakami, and S. Sawaki, "Comparison of various revised k-ε models and LES applied to flow around a high-rise building model with 1:1:2 shape placed within the surface boundary layer," *Journal of Wind Engineering and Industrial Aerodynamics*, vol. 96, no. 4, 2008, doi: 10.1016/j.jweia.2008.01.004.

[14] A. Abd Razak, A. Hagishima, N. Ikegaya, and J. Tanimoto, "Analysis of airflow over building arrays for assessment of urban wind environment," *Build Environ*, vol. 59, 2013, doi: 10.1016/j.buildenv.2012.08.007.

[15] N. Ikegaya, Y. Ikeda, A. Hagishima, A. A. Razak, and J. Tanimoto, "A prediction model for wind speed ratios at pedestrian level with simplified urban canopies," *Theor Appl Climatol*, vol. 127, no. 3–4, 2017, doi: 10.1007/s00704-015-1655-z.

[16] N. Ikegaya, T. Okaze, H. Kikumoto, M. Imano, H. Ono, and Y. Tominaga, "Effect of the numerical viscosity on reproduction of mean and turbulent flow fields in the case of a 1:1:2 single block model," *Journal of Wind Engineering and Industrial Aerodynamics*, vol. 191, pp. 279–296, Aug. 2019, doi: 10.1016/j.jweia.2019.06.013.

[17] T. Okaze et al., "Large-eddy simulation of flow around an isolated building: A step-by-step analysis of influencing factors on turbulent statistics," *Build Environ*, vol. 202, Sep. 2021, doi: 10.1016/j.buildenv.2021.108021.

[18] W. Wang, N. Ikegaya, and T. Okaze, "Comparing Weibull distribution method and Gram–Charlier series method within the context of estimating low-occurrence strong wind speed of idealized building cases," *Journal of Wind Engineering and Industrial Aerodynamics*, vol. 236, 2023, doi: 10.1016/j.jweia.2023.105401.

[19] F. Li, C. Hirose, W. Wang, C. H. Liu, and N. Ikegaya, "Correlations among high-order statistics and low-occurrence wind speeds within a simplified urban canopy based on particle image velocimetry datasets," *Build Environ*, vol. 247, 2024, doi: 10.1016/j.buildenv.2023.111050.

[20] Architectural Institute of Japan, *Guidebook for Practical Applications of CFD to Pedestrian Wind Environment around Buildings*. 2007.

[21] OpenCFD Ltd, "OpenFOAM User Guide 2016." [Online]. Available: https://www.openfoam.com/.

[22] S. Murakami, A. Mochida, and S. Sakamoto, "CFD analysis of wind-structure interaction for oscillating square cylinders," *Journal of Wind Engineering and Industrial Aerodynamics*, vol. 72, no. 1–3, 1997, doi: 10.1016/S0167-6105(97)00245-6.

[23] M. Kuroda, T. Tamura, and M. Suzuki, "Applicability of LES to the turbulent wake of a rectangular cylinder-Comparison with PIV data," *Journal of Wind Engineering and Industrial Aerodynamics*, vol. 95, no. 9–11, 2007, doi: 10.1016/j.jweia.2007.02.004.

[24] H. Ono, H. Takimoto, T. Michioka, and A. Sato, "CONVECTION TERM DISCRETIZATION FOR LARGE EDDY SIMULATIONS BASED ON THE FINITE VOLUME METHOD," *Journal of Environmental Engineering (Transactions of AIJ)*, vol. 80, no. 718, 2015, doi: 10.3130/aije.80.1143.

[25] S. M. Salim, R. Buccolieri, A. Chan, and S. Di Sabatino, "Numerical simulation of atmospheric pollutant dispersion in an urban street canyon:

Comparison between RANS and LES," *Journal of Wind Engineering and Industrial Aerodynamics*, vol. 99, no. 2–3, 2011, doi: 10.1016/j.jweia.2010.12.002.

[26] H. Tanaka, R. Yoshie, and C. Hu, "Uncertainty in Measurements of Velocity and Concentration around a Building," *The 4th International Symposium on Computational Wind Engineering*, vol. 4, no. Figure 1, 2006.

[27] Tokyo Polytechnic University, "Database on Outdoor Air Pollution." [Online]. Available: http://www.wind.arch.t-kougei.ac.jp/info_center/pollution/Isothermal_Flow.html

[28] J. Smagorinsky, "GENERAL CIRCULATION EXPERIMENTS WITH THE PRIMITIVE EQUATIONS," *Mon Weather Rev*, vol. 91, no. 3, 1963, doi: 10.1175/1520-0493(1963)091<0099:gcewtp>2.3.co;2.

[29] H. K. Versteeg, W. Malalasekera, G. Orsi, J. H. Ferziger, A. W. Date, and J. D. Anderson, *An Introduction to Computational Fluid Dynamics - The Finite Volume Method*. 1995.

[30] W. Wang and T. Okaze, "Statistical analysis of low-occurrence strong wind speeds at the pedestrian level around a simplified building based on the Weibull distribution," *Build Environ*, vol. 209, 2022, doi: 10.1016/j.buildenv.2021.108644.

[31] W. Wang, K. Seta, and N. Ikegaya, "Modelling probability density functions based on the Gram–Charlier series with higher-order statistics: Theoretical derivation and application," *Journal of Wind Engineering and Industrial Aerodynamics*, vol. 231, 2022, doi: 10.1016/j.jweia.2022.105227.